Dynamics of wetting with nonideal surfaces. The single defect problem

E. Raphaël and P. G. de Gennes
Collège de France, Physique de la Matière Condensée, 11, place Marcelin-Berthelot, 75231 Paris, Cedex 05, France

(Received 15 February 1989; accepted 10 March 1989)

Under static conditions, the macroscopic contact angle θ between a (partially wetting) liquid, a solid, and air, lies between two limiting values θ_r (receding) and θ_a (advancing). If we go beyond these limits (e.g., $\theta = \theta_a + \epsilon$, $\epsilon > 0$) the contact line moves with a certain macroscopic velocity $U(\epsilon)$. In the present paper, we discuss $U(\epsilon)$ (at small ϵ) for a very special situation where the contact line interacts only with one defect at a time. (This could be achieved inside a very thin capillary, of radius smaller than the average distance between defects.) Using earlier results on the elasticity and dynamics of the contact line in ideal conditions, we can describe the motions around "smooth" defects (where the local wettability does not change abruptly from point to point). For the single defect problem in a capillary, two nonequivalent experiments can be performed: (a) the *force* F is imposed (e.g., by the weight of the liquid column in the capillary). Here we define $\epsilon = (F - F_m)/F_m$, where F_m is the maximum pinning force which one defect can provide. We are led to a time averaged velocity $\overline{U} \sim \epsilon^{1/2}$. (b) The *velocity* U is imposed (e.g., by moving a horizontal column with a piston). Here the threshold force is not at $F = F_m$, but at a lower value $F = F_U$—obtained when the contact line, after moving through the defect, leaves it abruptly. Defining $\overline{\epsilon} = (\overline{F} - F_U)/F_U$, where $\overline{F}$ is the time average of the force, we find here $U \sim \overline{\epsilon}^{3/2}$. These conclusions are strictly restricted to the single defect problem (and to smooth defects). In practical situations, the contact line couples simultaneously to many defects: the resulting averages probably suppress the distinction between fixed force and fixed velocity.

I. INTRODUCTION

A. Motions on ideal surfaces

On a flat, homogeneous, surface, a partially wetting liquid reaches an equilibrium contact angle θ_0 defined by the Young condition.[1] If we impose a slightly different angle $\theta = \theta_0 + \epsilon$, the contact line moves with a velocity U. The relation between U and ϵ can be understood in rather simple terms[2]: the entropy source (the dissipation per unit length of line) is

$$T\mathring{S} = F_y U = \gamma(\cos\theta - \cos\theta_0)\, U\,, \tag{1.1}$$

where F_y is the unbalanced Young force (γ being the surface tension). In situations of partial wetting (where there is no precursor film[3]), the main dissipation is due to macroscopic flow. At small U, the fluid profile is nearly static and is a simple wedge of angle θ_0: for general θ_0, this dissipation has been calculated.[4] For small θ (which will turn out to be the most interesting case), the hydrodynamic dissipation has a simple form[5]:

$$T\mathring{S} = 3\,\frac{\eta U^2}{\theta}\, l\,, \tag{1.2}$$

where η is the fluid velocity, and l a logarithmic factor: $l = \ln(x_{\max}/x_{\min})$. Here $x_{\max}$ is the distance (from the contact line) at which the dynamic angle θ is measured, and $x_{\min}$ is a cut off at small distances. Most of the theoretical work performed in mechanics departments tends to describe $x_{\min}$ in terms of a slippage at the solid surface. This leads to $x_{\min} \sim a/\theta$ (a molecular size). On the other hand, long range Van der Waals forces modify the wedge profile over a much longer length a/θ^2 and suppress the singularity.[3,5] Thus Van der Waals forces dominate at small θ and $x_{\min} \sim a/\theta^2$. More generally, the dissipation by hydrodynamic losses is dominant only at θ small: we shall always assume $\theta \ll 1$ in what follows.

Equating the forms (1.1) and (1.2) for the dissipation, and specializing to small angles and low velocities, we get

$$U = \frac{\gamma}{3l\eta}\,\theta_0\,\frac{1}{2}(\theta^2 - \theta_0^2) \simeq \frac{\gamma\theta_0^2}{3l\eta}\,\epsilon \tag{1.3}$$

($\epsilon \ll \theta_0$).
Thus, for the ideal case, the relation between the force F (proportional to ϵ) and the velocity U is *linear*.

B. Anchoring defects

Practical surfaces have two types of defects: surface roughness and chemical contamination. The latter can be described in terms of a local modulation of the interfacial energies γ_{SL} (between solid and liquid) and γ_{SO} (between solid and air). The combination of interest is[6]

$$-h(x,y) = \gamma_{SL}(x,y) - \gamma_{SO}(x,y) - (\gamma_{SL} - \gamma_{SO})_0\,, \tag{1.4}$$

where x,y specify a point on the surface, and the bracket $(\ )_0$ denotes the unperturbed value. We shall be concerned with defects associated with a function h which is *localized* (a small spot of characteristic size d) and *smooth* (no discontinuities in h): a typical example being a Gaussian shape for $h(x,y)$. We assume that our defects are *dilute* (the distance between them is much larger than d). As shown in Ref. 6, the effects of surface roughness can also be described in terms of an h function.

 0021-9606/89/127577-08$02.10

The anchoring of a contact line on a single, smooth defect was analyzed in detail in Ref. 6. An essential ingredient is the *elasticity* of the contact line, which differs strikingly from the behavior of a violin string, as explained on Fig. 1. However, if the line is pinched at one point (say near a defect), and thus displaced from its average position y_L up to a local position y_m, there is a (nearly) hookean restoring force, of magnitude.

$$f_r = k(y_m - y_L)\,, \tag{1.5}$$

where

$$k = \frac{\pi\gamma\theta_0^2}{\ln L/d}\,. \tag{1.6}$$

Here L is the overall length of line involved, and d is the size of the anchoring defect. The force f_r must be balanced by the force f from the defect.

$$f(y_m) \simeq \int_{-\infty}^{+\infty} dx\, h(x,y_m)\,. \tag{1.7}$$

Equating Eqs. (1.5) and (1.7) one is led to the construction shown on Fig. 2. For a given position y_L of the line far from the defect, one can thus find one (or more) equilibrium positions for the anchoring point y_m.

When the amplitude of the h function is small, there is only one root y_m at any given y_L; we call this the weak defect regime. Reference 6 shows that in this regime (with many defects, but well separated and weak), we expect *no hysteresis*; if we move the line adiabatically (y_L increasing slowly with time) the position y_m is a smooth function of y_L and thus a smooth function of time: no special disssipation occurs when passing a defect. On the other hand, if we are in the strong defect regime, at some moment (when $y_L = Y_+$ on Fig. 2) the central point (y_m) jumps from an anchored position to a nearly unperturbed position ($y_m \sim y_L$): this jump causes an irreversible dissipation.

C. Relaxation of a pinched contact line

The relaxation modes of a contact line on an ideal surface have been analyzed in Ref. 7. This is done in two steps:

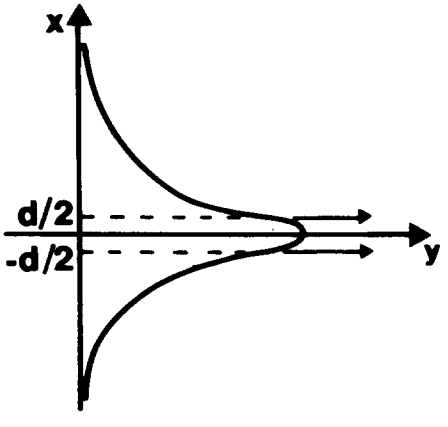

FIG. 1. Distortion of the contact line induced by a localized force acting over a distance d (under such a force, a violin string would be distorted into two straight segments).

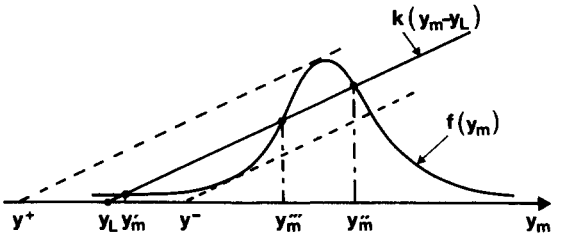

FIG. 2. Equilibrium positions of the anchoring point ($y = y_m$) of the line on the defect. For a given nominal line position (y_L), there may be three equilibrium positions, two of these (y_m', y_m'') are locally stable. When $y_L = Y_+$, y_m jumps from an anchored position to a nearly unperturbed position. We call F_U the force exerted by the defect at the threshold $y_L = Y_+$.

(a) deriving a local restoring force for a distorted line, from the elastic theory of Ref. 6. (b) using an analog of Eq. (1.3) giving the local velocity in terms of the driving force. The result is a set of relaxation modes, for each wave vector q, with rates

$$\frac{1}{\tau_q} = \frac{\gamma\theta_0^3}{3l\eta}|q| \quad (\theta_0 < 1)\,. \tag{1.8}$$

An important application of these ideas is the *release of a pinched string*: at times $t < 0$, the contact line is pulled locally with a force $f\delta(x)$, and reaches the logarithmic equilibrium shape shown on Fig. 1. At $t = 0$ the force is suppressed, and Eq. (1.8) leads to a transient shape:

$$y(x,t) = -\frac{f}{2\pi\gamma\theta_0^2}\ln(x^2 + c^2t^2) + \text{const.}\,, \tag{1.9}$$

where the velocity c is defined by

$$c = \frac{\gamma\theta_0^3}{3l\eta} \quad (\theta_0 < 1) \tag{1.10}$$

and is very sensitive to the magnitude of the equilibrium angle θ_0. Equation (1.9) shows that a portion (of length $2ct$) of the pinched string, relaxes, while the outer parts ($|x| > ct$) are essentially unperturbed. These results will be useful when we describe a line separating from an anchoring defect, in the following sections.

II. SIMPLIFIED DYNAMICAL EQUATIONS

A. Fixed force

Our aim is now to describe motions of the contact line, not on an ideal surface, but in the presence of a defect. The methods follows Ref. 6: we do not describe the whole profile $y(x,t)$, but reduce it to two variables (Fig. 3) (a) the global position of the line $y_L(t)$, (b) the position of the tip $y_m(t)$.

Consider for instance a vertical capillary, of diameter R, containing a liquid column of height $H \gg R$. The driving force $F = \pi R^2 H\rho g$ is thus imposed (ρ = liquid density, g = gravitational acceleration).

If the total weight F is smaller than the maximum pinning force

$$F_m = f(y_d) \tag{2.a}$$

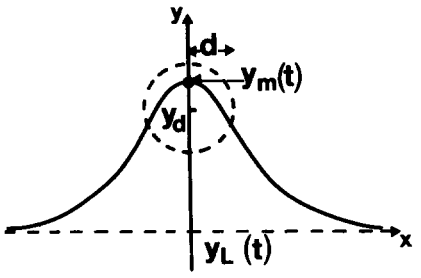

FIG. 3. A contact line anchored on a defect (of size d). A time t, the profile is characterized by the global position of the line [$y_L(t)$] and by the position of the tip [$y_m(t)$].

which one defect can provide, the column is at rest, the gravity force being balanced by the force of the defect. The equilibrium values of y_L and y_m may be deduced from a simple graphical construction (see Fig. 4). For $F = F_m$, the equilibrium value of y_m coincides with y_d (y_d specifying the "center" of the defect).

We now assume that the driving force F is slightly larger than the threshold value F_m:

$$F = F_m(1+\epsilon) \quad (0<\epsilon\ll 1)\,. \tag{2.b}$$

The balance of forces is not possible any more and the fluid moves down the capillary (Fig. 5). The global velocity is

$$\frac{dy_L}{dt} = \mu_L\left[k(y_m - y_L) - \tilde{F}\right]. \tag{2.1}$$

Here μ_L is a mobility (ratio of velocity/total force) for the $q=0$ mode, which we derive from Eqs. (1.1) and (1.2):

$$\mu_L = \frac{1}{2\pi R}\frac{\theta}{3\eta l}. \tag{2.2}$$

The force [the bracket in Eq. (2.1)] contains two terms: the first $k(y_m - y_L)$ is the spring force, with k defined in Eq. (1.6). The second term $\tilde{F}$ is *not* the total weight F for the following reason: as soon as the whole column starts moving down ($dy_L/dt \neq 0$) we have an important Poiseuille dissipation inside the whole column, and a resulting pressure drop.

This leads to

$$\tilde{F} = \pi R^2 H\left(\rho g + 8\frac{\eta}{R^2}\frac{dy_L}{dt}\right). \tag{2.3}$$

Inserting Eq. (2.3) into (2.1) we arrive at

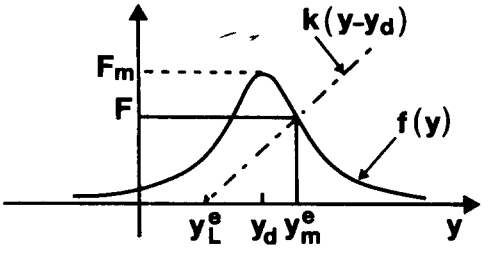

FIG. 4. Geometrical construction for the equilibrium position of the contact line (y_L^e) and of the tip (y_m^e). F is the total weight of the liquid column.

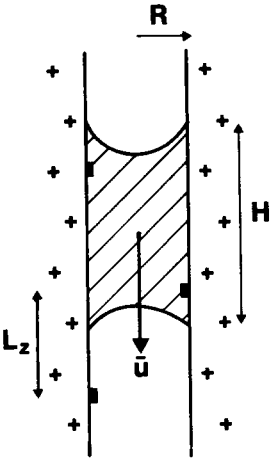

FIG. 5. A column of liquid, of height H, moving down a vertical capillary with a time averaged velocity $\bar{U}$. The black patches represent chemical contamination of the inner capillary surface. The average distance L_z between the defects is much greater than the capillary radius R.

$$\frac{dy_L}{dt} = \mu_0[k(y_m - y_L) - F]\,, \tag{2.4}$$

where μ_0 is a renormalized mobility.

$$\mu_0^{-1} = \mu_L^{-1} + 8\pi\eta H\,. \tag{2.5}$$

In the limit of interest ($H \gg R$) the Poiseuille term dominates:

$$\mu_0 \simeq \frac{1}{8\pi\eta H} \tag{2.6}$$

Equations (2.4) and (2.6) specify the global motion. Let us now discuss the motion of the tip. We write

$$\frac{dy_m}{dt} = \mu_m[k(y_L - y_m) + f(y_m - y_d)]\,. \tag{2.7}$$

Here μ_m is a mobility for modes of high wave vector q. Returning to Eq. (1.8), we see that $\mu_m \sim$ const. $\theta q/\eta$. The q values of interest near the tip are of order d^{-1} (where d is the defect size). Thus we write

$$\mu_m = \text{const.}\frac{\theta}{\eta d}\,. \tag{2.8}$$

This estimate of μ_m is correct for a tip which is just being unhooked, and is thin ($\sim d$). After separation, the tip gets more diffuse [see Eq. (1.9)] and the mobility is expected to decrease. However, we shall see that the crucial step is at the onset of separation, and thus the choice (2.8) is reasonable.

Returning to Eq. (2.7), we find in the bracket two forces: first the spring force, and second the force f due to the defect [Eq. (1.7)]. This force depends on the distance between tip and defect $y_m - y_d$.

To summarize: the dynamics for fixed force is specified in terms of two equations (2.4) and (2.7). These equations are highly nonlinear via the defect force $f(y_m - y_d)$. Their solutions will be discussed in Sec. III.

B. Fixed velocity

We now consider a different experiment (Fig. 6) where the liquid is horizontal (no gravity force) and pushed by a piston at constant speed U. We sit in the reference frame of

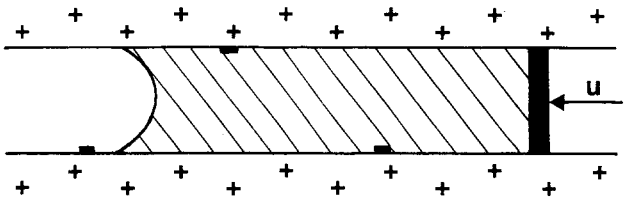

FIG. 6. A column of liquid in a horizontal capillary. The liquid is pushed by a piston at constant speed U. The black patches represent chemical contamination of the inner capillary surface.

the piston: thus $y_L(t) =$ constant (and we choose $y_L = 0$). We are left with a single variable of interest:

$$s = y_m - y_L \,. \tag{2.9}$$

The position of the defect is $y_d = Ut$, and the basic dynamical equation is

$$\frac{ds}{dt} = -\mu_m k s + \mu_m f(s - Ut) \,, \tag{2.10}$$

again highly nonlinear.

We shall discuss $s(t)$ in Sec. IV. Once $s(t)$ is determined, we know the instantaneous force due to the defect:

$$F(t) = ks(t) \,. \tag{2.11}$$

The total force experienced by the piston is the sum of $F(t)$ and of a Poiseuille term (linear in U) which is not interesting for us. Our main aim here is to compute the time average of $F(t)$ when the contact line passes a sequence of well separated defects (one at a time!).

III. DYNAMICS FOR FIXED FORCE

A. Adiabatic approximation

We now return to Eqs. (2.4) and (2.7) which describe the dynamics of the fixed force experiment. Introducing the new variables:

$$x = y_d - y_m \tag{3.1}$$

$$s = y_m - y_L \tag{3.2}$$

these two equations can be rearranged as

$$\frac{dx}{dt} = \mu_m [ks - f(x)] \tag{3.3}$$

$$\frac{ds}{dt} = -\frac{s}{t_1} + \mu_0 F + \mu_m f(x) \,, \tag{3.4}$$

where the time t_1 is defined by

$$\frac{1}{t_1} = k(\mu_0 + \mu_m) \,. \tag{3.5}$$

An approximate solution to Eq. (3.4) is obtained by setting the left-hand side of Eq. (3.4) equal to zero (*adiabatic approximation*). This leads to

$$s = t_1[\mu_0 F + \mu_m f(x)] \,. \tag{3.6}$$

Inserting Eq. (3.6) into Eq. (3.3) we get

$$\frac{dx}{dt} = \tilde{\mu}[F - f(x)] \,, \tag{3.7}$$

where $\tilde{\mu}$ is a renormalized mobility:

$$\tilde{\mu} = \frac{\mu_0 \mu_m}{\mu_0 + \mu_m} \,. \tag{3.8}$$

Since $\mu_m \gg \mu_0$, $\tilde{\mu}$ differs only slightly from μ_0.

To estimate the range of validity of the adiabatic approximation, we have to calculate the ratio:

$$r = \frac{|ds/dt|}{s/t_1} \tag{3.9}$$

for the solution (3.6). Using Eqs. (3.6) and (3.7), we get

$$r = \frac{t_1 \mu_m \tilde{\mu} \left| \frac{df}{dx} \right| (F - f)}{\mu_0 F + \mu_m f} \,. \tag{3.10}$$

The above expression can be easily evaluated; in the Gaussian model, for instance, one finds

$$r \approx \frac{h_0}{\gamma\theta^2} \frac{d}{\theta H} \,. \tag{3.11}$$

Here h_0 characterizes the defect strength [see Eq. (1.5)]:

$$h(x,y) = h_0 \exp - (x^2 + y^2)/2d^2 \tag{3.12}$$

and is of the order of $\gamma\theta^2$. Thus, in the limit of interest ($H \gg d$), Eq. (3.11) leads to very small values of r ($r \ll 1$). Therefore, the adiabatic approximation is valid everywhere.

Thus the motion is described by Eqs. (3.7) and (3.6). As we shall see now, this leads to plots of $x(t)$ and $s(t)$ which are *smooth* functions of time.

B. Macroscopic velocity

We now want to compute the time averaged velocity $\bar{U}$ of the liquid column within the framework of the adiabatic approximation. The defects are assumed to be identical, and spread at random on the (inner) capillary surface (Fig. 5). If we call n the number of defects per cm^2, the average (vertical) distance L_z between defects is given by

$$2\pi R L_z n = 1 \,. \tag{3.13}$$

We assume that L_z is much greater than the capillary radius R ($L_z \gg R$) so that the contact line interacts only with one defect at a time.

The typical time $t(L_z)$ required by the tip to cover the distance L_z around one defect is given by [see Eq. (3.7)]

$$t(L_z) = \int_{-L_z/2}^{+L_z/2} dx \frac{1}{\tilde{\mu}[F - f(x)]} \,. \tag{3.14}$$

For a Gaussian defect [Eq. (3.12)], the force (1.7) exerted by the defect is also Gaussian:

$$f(x) = F_m \exp - (x^2/2d^2) \tag{3.15}$$

For that case, Eq. (3.14) leads to

$$t(L_z) \cong \frac{\sqrt{2\pi} d}{\tilde{\mu} F_m} \epsilon^{-1/2} \,. \tag{3.16}$$

The time averaged velocity $\bar{U}$ is simply defined by

$$\bar{U} = \frac{L_z}{t(L_z)} \,. \tag{3.17}$$

Inserting Eq. (3.16) into (3.17) we are led to

$$\overline{U} \sim \frac{1}{nRH}\left(\frac{h_0}{\eta}\right)\epsilon^{1/2} \quad [\epsilon \ll (d/L_z)^2] \tag{3.18}$$

For $\epsilon > (d/L_z)^2$, the contact line velocity is given by the Poiseville velocity: $F_m(1+\epsilon)/8\pi\eta H$.

IV. DYNAMICS FOR FIXED VELOCITY

A. The quasistatic distortion

We now consider the fixed velocity experiment of Fig. 6; the dynamics is specified by Eq. (2.10). In what follows, we shall always take the piston speed U to be small. The quasistatic distortion $s_a(t)$ is obtained by setting the left-hand side of Eq. (2.10) equal to zero. This leads to

$$s_a = t_2 \mu_m f(s_a - Ut)\,, \tag{4.1}$$

where the time t_2 is defined by

$$\frac{1}{t_2} = k\mu_m\,. \tag{4.2}$$

A schematic plot of s_a as a function of time is shown in Fig. 7. In the strong pinning regime s_a is a *multivalued* function of t; it jumps abruptly (from s_d to s^+) at $t = t_d$.

B. The perturbative expansion

Far away from the "disanchoring point" (t_d, s_d), (i.e., for $t \ll t_d$), we can solve Eq. (2.10) perturbatively by expanding $s - s_a$ in powers of U:

$$s(t) = s_a(t) + U\sigma_1(t) + U^2\sigma_2(t) + \cdots\,, \tag{4.3}$$

where the $\sigma_i(t)$ are of order 1. Substituting Eq. (4.3) into Eq. (2.10), we obtain for the leading correction to s_a:

$$\sigma_1(t) = t_2 \frac{k^{-1}f'(s_a - Ut)}{1 - k^{-1}f'(s_a - Ut)}\,. \tag{4.4}$$

Note that the sign of $\sigma_1(t)$ changes for $t = t_{\max}$ (see Fig. 7).

C. Behavior near the disanchoring point

We now want to study the behavior of $s(t)$ near the disanchoring point. In that region, the preceding expansion (4.3) becomes invalid. However, in this region Eq. (2.10) can be approximated by the simpler form:

$$\frac{d\mu}{d\theta} = -\frac{U}{t_2}\theta - c\mu^2\,, \tag{4.5}$$

where we have introduced the new variables:

$$\theta = t - t_d \tag{4.6}$$

$$\mu = s - s_d\,. \tag{4.7}$$

Here c is a constant defined by

$$c = \frac{1}{2}\mu_m |f''(s_d - Ut_d)| \approx \frac{1}{dt_2}\,. \tag{4.8}$$

Equation (4.5) can be scaled by introducing

$$\theta = \alpha\tilde{\theta} \tag{4.9}$$

$$\mu = \beta\tilde{\mu} \tag{4.10}$$

with

$$\alpha = \left(\frac{t_2}{cU}\right)^{1/3} \sim t_2\left(\frac{d}{Ut_2}\right)^{1/3} \tag{4.11}$$

$$\beta = \frac{1}{c\alpha} \sim d\left(\frac{Ut_2}{d}\right)^{1/3}\,. \tag{4.12}$$

This leads to

$$\frac{d\tilde{\mu}}{d\tilde{\theta}} = -\tilde{\theta} - \tilde{\mu}^2\,. \tag{4.13}$$

Equation (4.13) is a Riccati equation which admits for general solution:

$$\tilde{\mu} = -\frac{A_i'(-\tilde{\theta}) + bB_i'(-\tilde{\theta})}{A_i(-\tilde{\theta}) + bB_i(-\tilde{\theta})}\,, \tag{4.14}$$

where A_i and B_i are the Airy functions,[8] A_i' and B_i' their derivatives; b is a constant of integration. To recover the quasi-static distortion:

$$\tilde{\mu}_a = +(-\tilde{\theta})^{1/2} \tag{4.15}$$

for large negative $\tilde{\theta}$, we must choose b equal to zero.[9] Whence

$$\tilde{\mu} = -\frac{A_i'(-\tilde{\theta})}{A_i(-\tilde{\theta})}\,. \tag{4.16}$$

The function $\tilde{\mu}$ is plotted in Fig. 8. At a value $\tilde{\theta}'' \simeq 2.339$ [corresponding to the first zero of the function $A_i(-\tilde{\theta})$], the function $\tilde{\mu}$ [Eq. (4.16)] diverges; the line separates from the defect. The simplified equation (4.5) ceases then to be valid.

To describe the late stages of the separation $(t > t'' = t_d + \alpha\tilde{\theta}'')$, we can approximate the term $f(s - Ut)$ of Eq. (2.10) by $f(s_a - Ut)$ where s_a now corresponds to the lower branch of Fig. 7. Neglecting the explicit time dependence of s_a this leads to

$$s(t) = \text{const.}\ \exp -\left(\frac{t}{t_2}\right) + s_a(t)\,. \tag{4.17}$$

Thus, the function s relaxes exponentially towards s_a in a time of order t_2. Note that this relaxation time is much smaller than α [Eq. (4.11)].

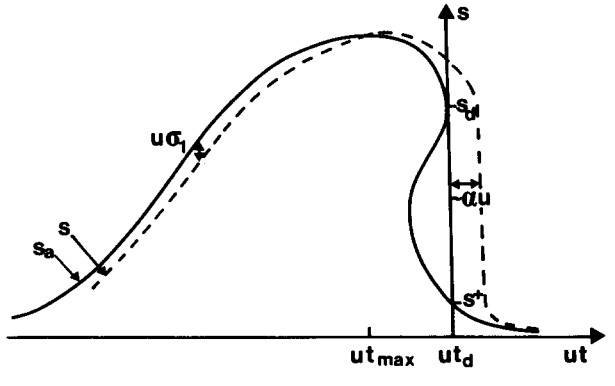

FIG. 7. Schematic plot of the quasistatic distortion s_a as a function of time (solid line). At $t = t_d$, s_a jumps abruptly from s_d to s^+. The dashed line represent the actual distortion $s(t)$ [Eq. (4.13)]. Note that the sign of the leading correction $U\sigma_1(t)$ to $s_a(t)$ changes at $t = t_{\max}$ where $s_a(t)$ is maximal.

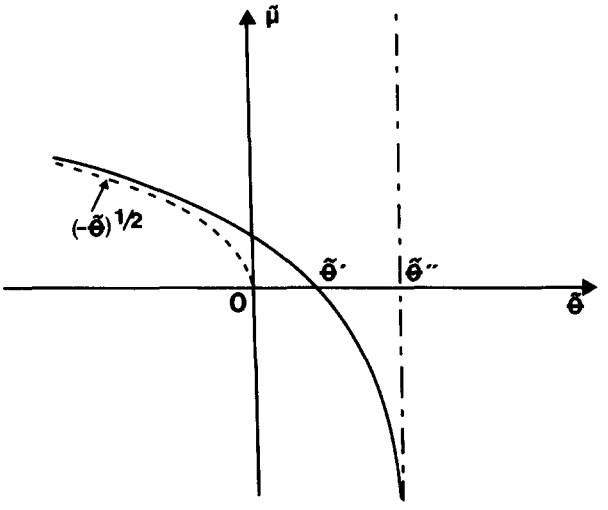

FIG. 8. Details of the disanchoring process $=\tilde{\mu}$ means the line position in reduced units [Eq. (4.10)] and $\tilde{\theta}$ is the reduced time [Eq. (4.9)]. At $\tilde{\theta}=\tilde{\theta}''$ the function $\tilde{\mu}$ diverges. The dashed line correspond to the quasi-staic solution $(-\tilde{\theta})^{1/2}$. For large negative $\tilde{\theta}$:$\tilde{\mu}\simeq(-\tilde{\theta})^{1/2}-(4\tilde{\theta})^{-1}$.

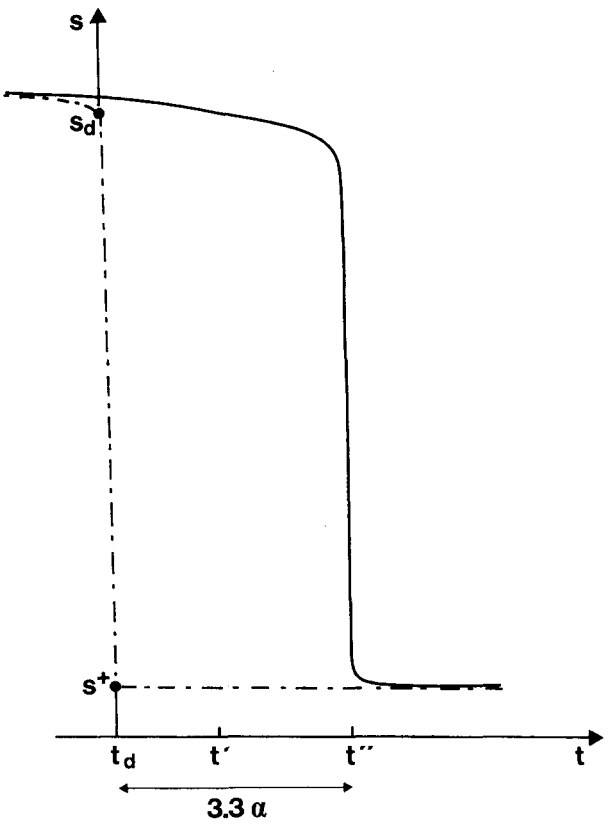

FIG. 9. Qualitative aspect of the line distortion $s(t)$ near the disanchoring point (t_d,s_d) (solid line). $s(t)$ differs markedly from the quasi-static distortion $s_a(t)$ (dashed line) only during the interval (t_d,t'') (of order 3.3 α). Between $t=t_d$ and $t=t''$ the function $s(t)$is almost flat except for the immediate vicinity of $t=t''$ where it jumps abruptly in a time of order t_2.

Let (t_r,s_r) be the coordinates of the crossover point between the two solutions (4.16) and (4.17). It is easy to see that t_r is contained between $t'=t_d+\alpha\tilde{\theta}'$ and $t''=t_d+\alpha\tilde{\theta}''$ [$\tilde{\theta}'$ corresponding to the first zero of the function $A_i'(-\tilde{\theta})$]. More precisely, it can be shown that

$$t''-t_r\simeq\sqrt{\frac{d}{s_d}}\,t_2\ll\alpha \tag{4.18}$$

and

$$\frac{s_d-s_r}{s_d}\simeq\sqrt{\frac{d}{s_d}}\ll 1\,. \tag{4.19}$$

A schematic representation of the behavior of $s(t)$ near $t=t_d$ is shown in Fig. 9. [Between $t=t_d$ and $t=t''$ the function $s_a(t)$ differs only slightly from the value $s^+\equiv s_a(t=t_d)$.]

The overall physical picture is the following:

- at times $t<t_d$ the contact line becomes progressively anchored — always remaining very close to its static conformation.

- at $t=t_d$ the line "springs off" and remains in the vicinity of the defect only for a time $\sim\alpha$.

- ultimately, the line relaxes to its unperturbed form in a (short) time t_2.

D. The time averaged force

We can now compute the time average of the instantaneous force (2.11):

$$\overline{F}=\frac{1}{T}\int_0^T ks(t)\,dt$$

$$=\frac{1}{T}\int_0^T ks_a(t)\,dt+\frac{1}{T}\int_0^T k\,[s(t)-s_a(t)]\,dt\,, \tag{4.20}$$

where the period T is defined by

$$UT=L_z\,. \tag{4.21}$$

Here L_z is the average distance between defects [see Eq. (3.13)]. By using Eq. (4.1), the first integral in Eq. (4.20) can be rewritten as an integral over the defect position y_d:

$$\frac{1}{T}\int_0^T ks_a(t)\,dt=\frac{1}{L_z}\int_{-L_z/2}^{+L_z/2} f(s_a-y_d)\,dy_d\,. \tag{4.22}$$

We may approximate the integral (4.22) by the simpler form:

$$2\pi nR\int_{-\infty}^{+\infty} f(s_a-y_d)\,dy_d\,. \tag{4.23}$$

This corresponds exactly to the static force derived in Ref. 6. In the present experiment this static force corresponds to F_U, the force obtained when the contact line, after moving through the defect, leaves it abruptly. (Note that F_U is smaller than F_m.) Thus we are led to

$$\overline{F}-F_U\simeq\frac{1}{T}\int_0^T k\,[s(t)-s_a(t)]\,dt\,. \tag{4.24}$$

The above integral can be easily evaluated by using the results of Sec. IV C. The dominant contribution comes from

the time (of order $3.3\,\alpha$) from t_d to t'' where $s - s_a$ is of the order of $s_d - s^+$ (see Figs. 7 and 9):

$$\int_0^T k\,[s(t) - s_a(t)]\,dt \sim k\alpha(s_d - s^+) \tag{4.25}$$

(where numerical factors have been ignored).
Inserting Eq. (4.25) into (4.24) we are led to

$$\bar{F} - F_U \sim F_m\left(1 - \frac{ks^+}{F_m}\right)(2\pi ndR)\left(\frac{Ut_2}{d}\right)^{2/3}. \tag{4.26}$$

In the strong defect regime, F_U differs only slightly from F_m. We therefore obtain, for fixed velocity,

$$U \sim \bar{\epsilon}^{\,3/2}, \tag{4.27}$$

where $\bar{\epsilon}$ is defined by

$$\bar{\epsilon} = \frac{\bar{F} - F_U}{F_U}. \tag{4.28}$$

V. CONCLUDING REMARKS

(1) The single defect problem which is discussed here is important, because it separates the mechanical factors from the statistical features which show up when the line interacts simultaneously with many defects. Clearly, if we want informations on one particular type of defect, associated with a certain surface treatment, the single defect situation is much more informative.

It is not hopeless to achieve this situation, either with a thin capillary, or with a fiber. Very recent experiments by J. M. di Meglio (to be published) monitor the force experienced by a thin fiber pulled at constant U, and do see erratic oscillations which may be due to separate defects.

(2) The great surprise which came out of our discussion is the distinction between fixed force and fixed velocity, leading to different thresholds F_c and to different laws near the threshold. For simple mechanical systems, differences of this type are in fact often observed: the analog of the disanchoring situation is seen in force experiments between two plates, as measured by the Israelachvili technique,[10] where we have competition between a spring force and a nonlinear attraction. On the other hand, the new machine built by J. M. Georges[11] measures the force at fixed interplate velocity.

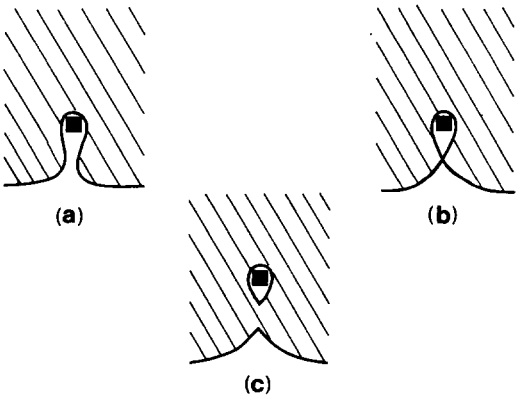

FIG. 10. A moving contact line anchored on a mesa defect (a). The disanchoring proceeds by the coalescence of two line portions (b). (Observations L. Léger and A. M. Guinet.)

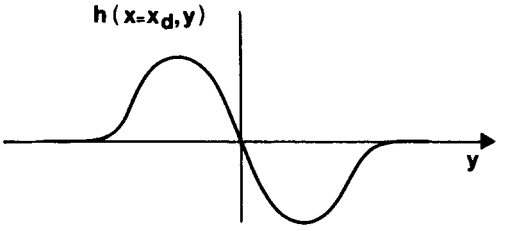

FIG. 11. General shape of the h function induced by a bump on the surface.

We hope to discuss the many defect situation in the future, and we expect a unique relation between force and velocity in this limit, where the contact line integrates simultaneous contributions from many defects, and averages them. However, this statistical problem is quite complex, as is already clear from its static counterpart[12] and many other surprises may occur.

(3) Returning to the single defect problem, we should repeat a severe limitation: we talked only about *smooth* defects. The opposite case of "mesa" defects seem to lead to very different structures, as observed recently by L. Léger and A. M. Guinet (unpublished). The disanchoring often proceeds here by coalescence of two line portions, as shown on Fig. 10. This process will be discussed separately.[13]

(4) Most of our figures, and of our numerical discussion, was based on "*chemical*" defects, where the h function is everywhere of the same sign. We should mention here the case of "*mechanical*" defects, where $h(x,y)$ is proportional to the local slope $\partial z/\partial y$ of the altitude profile $z(x,y)$ (see Ref. 6). The main difference is that a localized defect (a bump) gives an h function with the general aspect of Fig. 11, having now a maximum and a minimum of opposite signs. However, the distinction between weak and strong defects, the role of anchoring points, etc., remain the same, and we expect to retain the dynamical laws (3.18) and (4.27) when the defects are smooth bumps.

ACKNOWLEDGMENTS

We have benefited from stimulating discussions with F. Brochard, L. Léger, J. M. Di Meglio, J. F. Joanny, and M. Robbins.

[1] W. Zisman, in *Contact Angle, Wettability and Adhesion*, edited by F. M. Fowkes, Advances in Chemistry Series No. 43 (ACS, Washington, D.C., 1964).
[2] P. G. de Gennes, Colloid Polym. Sci. **264**, 463 (1986).
[3] P. G. de Gennes, Rev. Mod. Phys. **57**, 827 (1985).
[4] C. Huh and L. E. Scriven, J. Colloid Interface Sci. **35**, 85 (1971).
[5] P. Levinson, H. Xua, and P. G. de Gennes (to be published).

[7]P. G. de Gennes, C. R. Acad. Sci. (Paris) II **302**, 731 (1986).
[8](a) M. Abramowitz and I. A. Stegun, *Handbook of Mathematical Functions*, National Bureau of Standards (U.S. GPO, Washington, D.C.). (b) A somewhat similar analysis concerning the pinning of charge density waves may be found in D. Fisher, Phys. Rev. B **31**, 1396 (1985).
[9]If $b \neq 0$, the leading behavior of $\tilde{\mu}$ [Eq. (4.14)] for large negative $\tilde{\theta}$ is given by $\tilde{\mu} \approx -(-\tilde{\theta})^{1/2}$.
[10]J. N. Israelachvili and P. M. McGuiggan, Science **241**, 795 (1988).
[11]A. Tonck, J. M. Georges, and J. L. Loubet, J. Colloid Interface Sci. **126**, 150 (1988).
[12]J. F. Joanny and P. G. de Gennes, J. Chem. Phys. **81**, 552 (1984); M. O. Robbins and J. F. Joanny, Europhys. Lett. **3**, 729 (1987); M. Cieplak and M. O. Robbins, Phys. Rev. Lett. **60**, 2042 (1988); R. Bruinsma, to appear in Conference Proceedings of the European Physical Society Meeting, Arcachon, France, 1988.
[13]E. Raphael (to be published).